

ORIGINAL ARTICLE

Atypical Intrinsic Hemispheric Interaction Associated with Autism Spectrum Disorder Is Present within the First Year of Life

Max Rolison^{1,2}, Cheryl Lacadie¹, Katarzyna Chawarska^{2,3,4}, Marisa Spann⁵ and Dustin Scheinost^{1,2,3,6}

¹Department of Radiology and Biomedical Imaging, Yale School of Medicine, New Haven, CT 06520, USA, ²Child Study Center, Yale School of Medicine, New Haven, CT 06519, USA, ³Department of Statistics and Data Science, Yale University, New Haven, CT 06510, USA, ⁴Department of Pediatrics, Yale School of Medicine, New Haven, CT 06511, USA, ⁵Department of Psychiatry, Columbia University Irving Medical Center, New York, NY 10032, USA and ⁶Department of Biomedical Engineering, Yale University, New Haven, CT 06511, USA

Address correspondence to Dustin Scheinost, Magnetic Resonance Research Center, 300 Cedar St, PO Box 208043, New Haven, CT 06520-8043, USA. Email: dustin.scheinost@yale.edu

Abstract

Autism spectrum disorder (ASD) is characterized by atypical connectivity lateralization of functional networks. However, previous studies have not directly investigated if differences in specialization between ASD and typically developing (TD) peers are present in infancy, leaving the timing of onset of these differences relatively unknown. We studied the hemispheric asymmetries of connectivity in children with ASD and infants later meeting the diagnostic criteria for ASD. Analyses were performed in 733 children with ASD and TD peers and in 71 infants at high risk (HR) or normal risk (NR) for ASD, with data collected at 1 month and 9 months of age. Comparing children with ASD ($n = 301$) to TDs ($n = 432$), four regions demonstrated group differences in connectivity: posterior cingulate cortex (PCC), posterior superior temporal gyrus, extrastriate cortex, and anterior prefrontal cortex. At 1 month, none of these regions exhibited group differences between ASD ($n = 10$), HR-nonASD ($n = 15$), or NR ($n = 18$) infants. However, by 9 months, the PCC and extrastriate exhibited atypical connectivity in ASD ($n = 11$) and HR-nonASD infants ($n = 24$) compared to NR infants ($n = 22$). Connectivity did not correlate with symptoms in either sample. Our results demonstrate that differences in network asymmetries associated with ASD risk are observable prior to the age of a reliable clinical diagnosis.

Key words: data-driven, functional connectivity, functional MRI, resting-state

Introduction

Autism spectrum disorder (ASD) is a neurodevelopmental disorder that affects 1 in 54 children (Maenner et al. 2020). While the earliest behavioral symptoms of ASD manifest during the first year of life, diagnosis cannot be reliably made until the second year of life (Ozonoff et al. 2015). Thus, pioneering research is beginning to identify neural correlates of future diagnosis of

ASD in infants to understand how early atypical patterns in neural development may lead to the behavioral phenotype of ASD (Wolff et al. 2015; Eggebrecht et al. 2017; Emerson et al. 2017; Lewis et al. 2017; Shen et al. 2017).

Hemispheric specialization—the tendency for some neural processing to be asymmetrically localized to one hemisphere of the brain compared to the other—develops across the

life span, beginning in utero between the second and third trimesters (Dubois et al. 2009; Habas et al. 2012) and continuing throughout infancy and childhood (Fair et al. 2007). Atypical hemispheric asymmetries have been well demonstrated in children, adolescents, and young adults with ASD, which are generally observed as bilateral brain activation or reduced interhemispheric connectivity. These have been shown in auditory (Edgar et al. 2015), sensorimotor (Anderson et al. 2011; Floris et al. 2016), and language regions (Kleinhans et al. 2008; Redcay and Courchesne 2008), as well as in the default mode (Nielsen et al. 2014; Lee et al. 2016) and frontoparietal (Anderson et al. 2011; Cardinale et al. 2013) networks, and may underlie symptoms that are common among individuals with ASD (Floris et al. 2016, 2021; Lee et al. 2016). Thus, atypical hemispheric specialization may represent a potential neurological index of ASD which can be traced in individuals from a wide range of ages, yet no studies have investigated atypical specialization in the context of ASD across developmental ages and, particularly, in infants. It is not clear if the atypical patterns observed in school-age children represent a primary impairment in ASD or emerge over time secondary to other challenges present in ASD. Given the gap in age between the first appearance of behavioral symptoms of ASD in early toddlerhood and the neuroimaging work probing the hemispheric asymmetries in children, adolescents, and young adults with ASD, there remains a need to investigate when these patterns diverge between ASD and control groups. In other words, do the hemispheric specialization differences that characterize older individuals with ASD occur at younger ages—namely, in infancy, prior to the appearance of noticeable symptoms? For neurodevelopmental disorders, such as ASD, identifying early critical time periods for atypical brain development is paramount in elucidating etiological pathways that might contribute to the disorder.

Using cross-sectional and longitudinal data from multiple open-source datasets, we used functional magnetic resonance imaging (fMRI) to interrogate the degree to which brain networks preferentially interact with same (ipsilateral) as opposed to opposite (contralateral) hemispheres through resting-state functional connectivity (Wang et al. 2014), that is, the temporal correlation of brain activity. To do so, we used a data-driven, voxel-based approach—cross-hemisphere intrinsic connectivity distribution (chICD)—that has been previously validated in a range of disorders and conditions, including preterm birth (Scheinost et al. 2015) and schizophrenia (Scheinost et al. 2019). First, in a large cohort of school-age children ($n=733$) from the Autism Brain Imaging Data Exchange (ABIDE) sample, we investigated group differences in chICD. As chICD is a data-driven approach, we did not have an a priori hypothesis for which brain regions would exhibit atypical connectivity lateralization.

Next, using longitudinal infant data and the regions observed in the school-age cohort, we examined whether the same patterns are present, before reliable diagnosis, at 1 month and 9 months in 71 infants at high risk (HR) or normal risk (NR) for developing ASD. Nearly 20% of the siblings of children with ASD receive an ASD diagnosis (Ozonoff et al. 2011); thus, the study of infant siblings allows for the investigation of the earliest signs of ASD. Fifteen of these infants later met Autism Diagnostic Observation Schedule, second edition (ADOS-2) (Lord, Rutter et al. 2012) algorithm criteria for ASD. Given the early development of hemispheric specialization, we hypothesize that the neural correlates for the atypical asymmetry patterns observed in the school-age children begin to develop in infancy and, thus, will be observed in the

infant sample at 1 month of age. We hypothesize that the lateralization for the HR-nonASD infants will be in between those for the NR and ASD infants (i.e., $NR > HR\text{-nonASD} > ASD$).

Materials and Methods

Datasets

We used resting-state data obtained from ABIDE-I and ABIDE-II (Di Martino et al. 2014, 2017). All data were collected under the direction and approval of the respective institutions' ethics boards. Participants in our dataset included those ages 6–14 years. Participants were only included from sites where research-reliable clinicians administered the ADOS (Lord, Petkova, et al. 2012). Participants were administered the ADOS-G (Lord et al. 2002) (179 participants) and/or the ADOS-2 (Lord, Rutter et al. 2012) (239 participants). Participants with ASD had an established ASD diagnosis (average ADOS calibrated severity score 6.9). All participants had a full-scale intelligence quotient ($IQ \geq 70$). Typically developing (TD) participants did not have any psychiatric diagnoses, take any psychoactive medication, or have a family history of ASD. Magnetic resonance imaging (MRI) quality and preprocessing were assessed visually for registration accuracy and quantitatively for motion (see Motion Analysis). Participants from sites were only included in our analysis if at least 10 children in each diagnostic group from that site contributed usable data. Analyses included 301 children with ASD and 432 TD peers (see [Supplementary Table S1](#) for a list of included participants). As shown in [Supplementary Table S3](#), there were no differences in age between ASD and TD participants. While there was a difference in IQ (Cohen's $d=0.63$), all ASD participants had normal-range IQ scores with an average IQ of 105. There were 259 males and 42 females with ASD included, compared to 289 males and 143 TD females. There were 219 right-handed, 32 left-handed, and 41 mixed-handed children with ASD, compared to 375 right-handed, 20 left-handed, and 33 mixed-handed TD children. Handedness data were not available for nine children with ASD and four TD children.

Additionally, we used resting-state data obtained from the National Institute of Mental Health Data Archive (NDA) that was collected through the University of California Los Angeles Autism Center of Excellence (UCLA ACE) project. The dataset identifier is NDARCOL0002026. This dataset was chosen as it was the only dataset on NDA with both resting-state data at 1-month and follow-up ADOS testing. The sample consisted of 79 HR and NR infants with fMRI scans at 1–2 months and/or 9–10 months with resting-state data. HR is defined exclusively as a participant who has a biological sibling diagnosed with ASD. Five infants (four NR and one HR) were excluded for missing later diagnostic testing, and three HR infants were excluded for motion during scanning (see below).

Following the exclusions, we retained 40 (91%) and 31 (89%) of HR and NR infants, respectively. Out of the 71, 43 infants had data at 1–2 months, 57 infants had data at 9–10 months, and 29 infants had data at both (see [Supplementary Tables S4](#) and [S5](#)). ASD status was determined based on the results of the ADOS-2 evaluation. Twenty-one infants had data available from the administration of the ADOS-2 Toddler Module between 18 and 19 months. Toddlers whose scores fell into a “Moderate-to-Severe Concern” range were grouped into the ASD infant category ($n=2$; mean raw score = 19.0 ± 1.4). For

the remaining 50 infants, diagnostic classification was based on the ADOS-2, which was administered between 32 and 37 months. Toddlers with an overall calibrated severity score of ≥ 4 were grouped into the ASD infant category ($n=13$; mean = 5.9 ± 1.9). All participants were healthy, full-term infants following normal pregnancy with no complications. Scans were acquired during natural, nonsedated sleep. There were no differences in age ($P=0.2$) or sex ($P=0.6$) between the HR-nonASD and NR infants. However, only one infant grouped as ASD was female.

Imaging Parameters

For the ABIDE school-aged children, included data were collected at Kennedy Krieger Institute, Georgetown University, New York University, Oregon Health & Science University, University of California Los Angeles, University of Michigan, and Yale School of Medicine. Data acquisition parameters varied across sites. Details on scan parameter and site-specific protocols are available at http://fcon_1000.projects.nitrc.org/indi/abide/. Further information about how site was controlled for in analysis can be found below in Analytical Approach.

For the UCLA infants, included data were collected as part of the UCLA Autism Center of Excellence. Resting-state MRI were acquired at a 3 Tesla MR scanner (parameters: time repetition [TR]/time echo [TE]: 2000/28 ms, flip angle = 90° , FOV = 192 mm, 56×56 matrix, 34 axial 4-mm slices).

Common Space Registration

For the school-age children, anatomical images were skull-stripped using FSL and any remaining nonbrain tissue was manually removed. Next, to warp the functional images into Montreal Neurological Institute (MNI) space, a series of linear and nonlinear registrations were calculated independently and were combined into a single transform. This single transformation allows the single participant images to be transformed to common space with only one transformation, reducing interpolation error. Functional images were linearly registered to the anatomical image and the anatomical image was nonlinearly registered to the template MNI brain using a previously validated algorithm (Scheinost et al. 2017). For the infants, a mean functional image from the motion-corrected fMRI data (see below) was registered to a custom infant template (as given in Scheinost et al. (2016)) using the same validated algorithm (Scheinost et al. 2017).

Functional Connectivity Preprocessing

Functional data processing for school-age children and infants followed an identical pipeline. Functional images were slice-time- and motion-corrected using SPM8. Next, images were warped into common space using the transformation described above with cubic interpolation and were iteratively smoothed until the smoothness of any image had a full-width at half-maximum (FWHM) of approximately 6 mm using AFNI's 3dBlurToFWHM. This iterative smoothing reduces motion-related confounds (Scheinost et al. 2014). All further analyses were performed using BioImage Suite (Joshi et al. 2011) unless otherwise specified. Several covariates of no interest were regressed from the data, including linear and quadratic drifts, mean cerebral spinal fluid (CSF) signal, mean white matter

signal, and mean gray matter signal. For additional control of possible motion-related confounds, a 24-parameter motion model (including 6 rigid-body motion parameters, 6 temporal derivatives, and these terms squared) was regressed from the data. The data were temporally smoothed with a Gaussian filter (approximate cutoff frequency = 0.12 Hz). A canonical gray matter mask defined in common space was applied, so only voxels in the gray matter were used in further calculations.

Functional Connectivity Analysis

After standard functional connectivity preprocessing (see supplement, [Supplementary Fig. S1](#)), we examined the degree to which brain networks preferentially interact with same (ipsilateral) as opposed to opposite (contralateral) hemispheres through functional connectivity using chICD (Scheinost et al. 2015). Like other voxel-wise connectivity measures (Gotts et al. 2012; Tomasi and Volkow 2019), chICD involves correlating the time course for a voxel x with every other time course in the gray matter and then summarizing these correlations. However, chICD separates the contribution of each hemisphere to the overall connectivity, thereby providing a measure of the asymmetry of a voxel's connectivity.

Specifically, the time course for a voxel was correlated with the time course for every other voxel in the hemisphere ipsilateral to that voxel. ICD was used to model the distribution of these correlations. This procedure was performed for every voxel resulting in a map representing each voxel's connectivity within the same hemisphere, labeled as ICD(ipsi). Similarly, a map representing a voxel's connectivity to the contralateral hemisphere was calculated, labeled as ICD(contra). Both maps were normalized by subtracting the mean across all voxels and by dividing by the standard deviation across all voxels. This z-score-like normalization does not change the underlying connectivity pattern but allows for the investigation of relative differences in connectivity in the presence of large global differences in connectivity. Finally, to detect patterns of between hemisphere connectivity, the ICD(ipsi) and ICD(contra) maps were subtracted, creating our chICD metric: $\text{chICD} = \text{ICD}(\text{ipsi}) - \text{ICD}(\text{contra})$.

For single group chICD maps, a positive chICD value indicates stronger connectivity to the ipsilateral hemisphere (relative to both the mean ipsilateral connectivity and the contralateral connectivity). A negative chICD value indicates stronger connectivity to the contralateral hemisphere (relative to both the mean ipsilateral connectivity and the contralateral connectivity). This and similar procedures have been validated in several studies (Lee et al. 2014; Wang et al. 2014; Scheinost et al. 2015; 2019).

Follow-Up Seed Connectivity

As chICD summarizes connectivity differences across the whole brain into a single number, the specific connections that were most responsible for changes in connectivity are not readily observable. In school-age children, follow-up seed analysis was performed to explore post hoc the nodes identified by the chICD analysis to determine these specific connections. The time series of the seed region in each participant was then computed as the average time series across all voxels in the seed region. This time series was correlated with the time series for every other voxel in the gray matter to create a map of r -values, reflecting seed-to-whole-brain connectivity. These

R-values were transformed to z-values using Fisher's transform, yielding one map for each participant representing the strength of correlation to the seed region.

Motion Analysis

As group differences in motion have been shown to confound connectivity studies, we calculated the average frame-to-frame displacement for each participant's data. In line with current reports, participants with an average frame-to-frame displacement greater than 0.15 for any run were removed from the analysis for both the school-age and infant samples (school-age: 79 [21%] ASD and 42 [9%] TD; infants: 3 HR-nonASD, 0 NR, 0 ASD). Following the exclusions, motion was similar between the ASD and TD groups (ASD: 0.08 ± 0.03 , TD: 0.07 ± 0.03 , Cohen's $d = 0.27$) and between the HR-nonASD, NR, and ASD groups at 1 month (HR: 0.06 ± 0.02 , NR: 0.05 ± 0.03 , ASD: 0.05 ± 0.02 , Cohen's $f^2 = 0.02$) and 9 months (HR: 0.05 ± 0.03 , NR: 0.06 ± 0.03 , ASD: 0.06 ± 0.04 , Cohen's $f^2 = 0.01$). Finally, we regressed a 24-parameter motion model, used an iterative smoothing algorithm, and included motion as a covariate in group analyses for the school-age children to minimize any motion confounds (Satterthwaite et al. 2013; Scheinost et al. 2014).

Analytical Approach

For the school-aged children, chICD and seed connectivity data were analyzed with voxel-wise general linear modeling. Age, site, sex, IQ, and motion were included as covariates. Imaging results are shown at a cluster-level threshold of $P < 0.05$ family-wise error (FWE) correction as determined by AFNI's 3dClustSim program (version 16.0.09) using a cluster-forming threshold of $P \leq 0.001$, 10 000 iterations, a gray matter mask, and a smoothness estimated from the residuals using 3dFWHMx with the -ACF option. As a significant chICD difference could be driven by the differences in ipsilateral connectivity, contralateral connectivity, or both, post hoc two-sample t-tests (based on extracted chICD values from significant clusters) were used to test the direction of influence, corrected for multiple comparisons using Bonferroni correction.

For the infant sample, though we used voxel-wise comparisons in the larger school-age sample ($n = 733$), we chose only to test group differences based on ROIs from the school-age sample for two primary reasons. First, we explicitly wanted to determine whether the observed group differences in school-age children were observable in infancy. Second, the infant dataset had a much smaller sample size at each time point ($n < 60$), which reduces statistical power. ROI-based comparisons have higher power compared to voxel-wise comparison. To facilitate group comparisons, we warped the peak differences of the school-age results (in MNI space) into infant space using a transformation between the infant and MNI templates, estimated using the same validated algorithm as above. Once in infant space, 6-mm radius ROIs were created, centered on these peaks, which is consistent with ours and others' previous infant neuroimaging work (Scheinost et al. 2016; Rudolph et al. 2018). The average chICD values extracted using these ROIs from the infant chICD data were compared among the three groups using one-way ANOVAs. Finally, we compared developmental trajectories for the ROIs with significant group differences during infancy by contrasting the 9-month and 1-month data in infants with longitudinal data and by comparing these differences across groups.

Results

Connectivity Analysis

The chICD analysis revealed four clusters of altered hemispheric asymmetry of connectivity for children with ASD compared with TD peers ($P < 0.05$, corrected; Fig. 1 and Supplementary Fig. S3). Children with ASD demonstrated greater chICD in right posterior superior temporal gyrus (pSTG; R BA 22), indicating that this region more strongly interacts to the ipsilateral hemisphere in ASD. Also, children with ASD exhibited a more positive chICD value in the right extrastriate cortex (R BA 19). In the right anterior prefrontal cortex (PFC; R BA 10), children with ASD exhibited reduced chICD, indicating that this region more strongly interacts with the contralateral hemisphere in ASD. Finally, children with ASD demonstrated lower chICD in right posterior cingulate cortex (PCC; R BA 23/31), indicating that this region interacts weaker with the ipsilateral hemisphere. All regions exhibited medium effect sizes (pSTG: Cohen's $d = 0.49$, extrastriate: Cohen's $d = 0.32$, PCC: Cohen's $d = 0.41$, PFC: Cohen's $d = 0.65$).

Post hoc tests to evaluate the direction of chICD results suggest that the altered asymmetry in the right pSTG was due to weaker connectivity to the contralateral hemispheres in ASD (ASD vs. TD: ICD(ipsi) $t = -1.03$, $P = 0.31$, $df = 731$; ICD(contra) $t = -4.24$, $P < 0.001$, $df = 731$). In contrast to the pSTG finding, the asymmetry differences in the right extrastriate cortex were primarily due to greater connectivity to the ipsilateral hemispheres in ASD (ASD vs. TD: ICD(ipsi) $t = 3.31$, $P < 0.001$, $df = 731$; ICD(contra) $t = 1.61$, $P = 0.11$, $df = 731$). The right PCC differences in asymmetry were driven by weaker connectivity to the contralateral hemisphere compared to TD children (ASD vs. TD: ICD(ipsi) $t = -0.98$, $P = 0.34$, $df = 731$; ICD(contra) $t = -3.64$, $P < 0.001$, $df = 731$). Finally, in the right PFC, no significant difference connectivity to the ipsilateral and contralateral hemisphere in ASD relative to TD peers were observed (ASD vs. TD: ICD(ipsi) $t = -1.74$, $P = 0.08$, $df = 731$; ICD(contra) $t = -1.37$, $P = 0.17$, $df = 731$). These results are summarized in Supplementary Table S6.

Seed Connectivity

To further elucidate the differences in chICD between groups, follow-up seed connectivity analysis was performed with each of the four identified regions as seeds (Fig. 2). Connectivity from the PCC, extrastriate, and pSTG seeds showed standard default mode network (DMN) patterns for both groups (i.e., strong connectivity between the PCC, medial prefrontal cortex [mPFC], and bilateral angular gyri; Greicius et al. 2003); while connectivity from the PFC seed showed standard salience network patterns for both groups (i.e., strong connectivity between the dorsal anterior cingulate cortex [dACC] and bilateral insula; Seeley et al. 2007).

For children with ASD compared to TD peers, seed connectivity from right pSTG suggested that the reduced contralateral connectivity in ASD may be driven by weaker connectivity with left inferior frontal gyrus (IFG), left mPFC, and left visual association cortex as well as by greater connectivity with right fusiform and middle temporal gyrus. Seed connectivity from right extrastriate cortex revealed greater connectivity with right fusiform, middle temporal gyrus, and angular gyrus in children with ASD, which is consistent with the observed increased ipsilateral asymmetry. Seed connectivity from right PCC revealed weaker connectivity with right cerebellum, left PCC, left anterior PFC, left orbitofrontal area, left anterior cingulate cortex, and left IFG

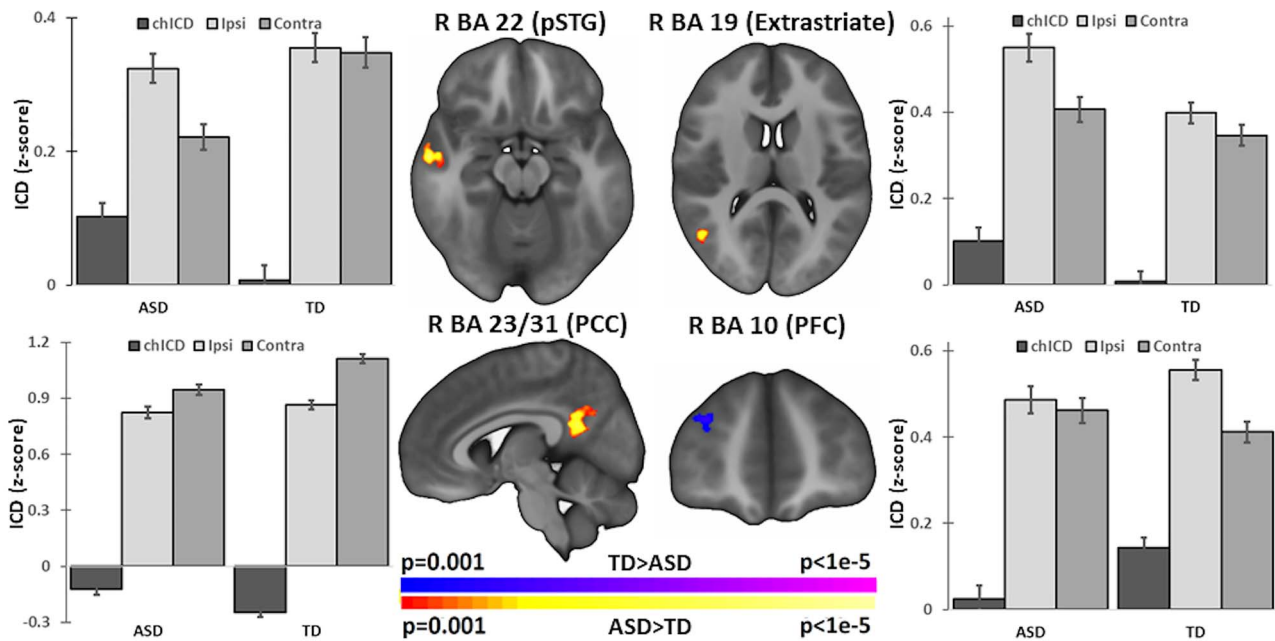


Figure 1. Group differences in connectivity hemispheric specialization at school-age. Group comparison (ASD vs. TD) identified four regions of atypical connectivity asymmetry: right pSTG (R BA 22), right extrastriate cortex (R BA 19), right PCC (R BA 23 and R BA 31), and right anterior PFC (R BA 10). Bar charts next to each image highlight the contribution of ipsilateral (ipsi) and contralateral (contra) connections to chICD differences. In other words, the plotted chICD values are the difference between the plotted ipsi and contra values. Error bars represent standard errors. Imaging results shown at $P < 0.05$ corrected and in radiologic convention.

and weaker negative connectivity with left insula and Broca's area, which is consistent with the observed weaker contralateral asymmetry in ASD. Seed connectivity from right anterior PFC revealed weaker connectivity with left putamen in children with ASD. Additionally, children with ASD demonstrated stronger connectivity with PCC.

Connectivity Differences in Infancy

At 1 month, no group differences were observed in the PCC, extrastriate, pSTG and PFC ROIs (Fig. 3A).

At 9 months, the chICD analysis revealed that two of the four regions (the PCC and the extrastriate) from the school-age sample exhibited group differences in chICD (Fig. 3B; PCC: $F = 4.01$, $P = 0.02$, $df = 2,47$; extrastriate: $F = 4.78$, $P = 0.01$, $df = 2,47$). No group differences were observed in the pSTG and PFC ROIs. In the right PCC, NR infants showed significantly stronger chICD compared to HR-nonASD and ASD infants (NR vs. HR-nonASD: $P = 0.02$, $t = 2.35$, $df = 44$, Cohen's $d = 0.69$; NR vs. ASD: $P = 0.03$, $t = 2.23$, $df = 31$, Cohen's $d = 0.79$; HR-nonASD vs. ASD: $P = 0.37$, $t = 0.92$, $df = 33$, Cohen's $d = 0.30$). In the right extrastriate, NR showed significantly weaker chICD compared to HR-nonASD and ASD infants (NR vs. HR-nonASD: $P = 0.03$, $t = -2.27$, $df = 44$, Cohen's $d = 0.67$; NR vs. ASD: $P = 0.01$, $t = -2.61$, $df = 31$, Cohen's $d = 0.96$; HR-nonASD vs. ASD: $P = 0.23$, $t = -1.22$, $df = 33$, Cohen's $d = 0.42$). In both regions, chICD for the HR-nonASD infants was in between those for the NR infants and the infants who later met ASD criteria. HR-nonASD did not differ significantly from the infants that later met ASD criteria. These results are also summarized in [Supplementary Table S7](#).

Finally, in the 29 participants (NR, $n = 13$; HR-nonASD, $n = 10$; ASD, $n = 6$) with data at both 1 and 9 months, we compared developmental trajectories using a repeated-measure ANOVA

for the extrastriate and PCC. We observed significantly different trajectories in the extrastriate chICD across groups ($F = 5.81$, $P = 0.008$, $df = 2,26$; Fig. 4A). Post hoc group comparisons with two-sample t-tests suggested this result was driven by a significant difference between the NR and ASD groups (NR vs. HR-nonASD: $P = 0.08$, $t = -1.85$, $df = 21$; NR vs. ASD: $P = 0.007$, $t = -3.06$, $df = 17$; HR-nonASD vs. ASD: $P = 0.06$, $t = -2.01$, $df = 14$). NR infants exhibited a significant decrease in chICD from 1 to 9 months (NR: $P = 0.009$, $t = -3.1$, $df = 12$). By contrast, HR-nonASD showed no change in chICD and ASD infants exhibited a trend increase in chICD (HR-nonASD: $P = 0.42$, $t = -0.85$, $df = 9$; ASD: $P = 0.11$, $t = 1.94$, $df = 5$). No differences in trajectories for the PCC were detected (Fig. 4B).

Correlations with Behavioral Measures

There were no significant associations between the behavioral measures and patterns of atypical cerebral lateralization in the school-age or infant samples (all P s < 0.05). In the school-age children, atypical cerebral lateralization in the four identified regions was not associated with full-scale IQ. Among the children with ASD, ADOS CSS was not associated with patterns of lateralization. In the infant sample, patterns of atypical lateralization at 9 months of age were not associated with ADOS CSS scores at 36 months.

Discussion

Using data-driven approaches and two open-source datasets, we examined the hemispheric specialization of connectivity in ASD during syndromal (after symptoms appear) and prodromal (before symptoms appear) stages of the disorder. First, comparing school-age children with ASD to TD peers, children with

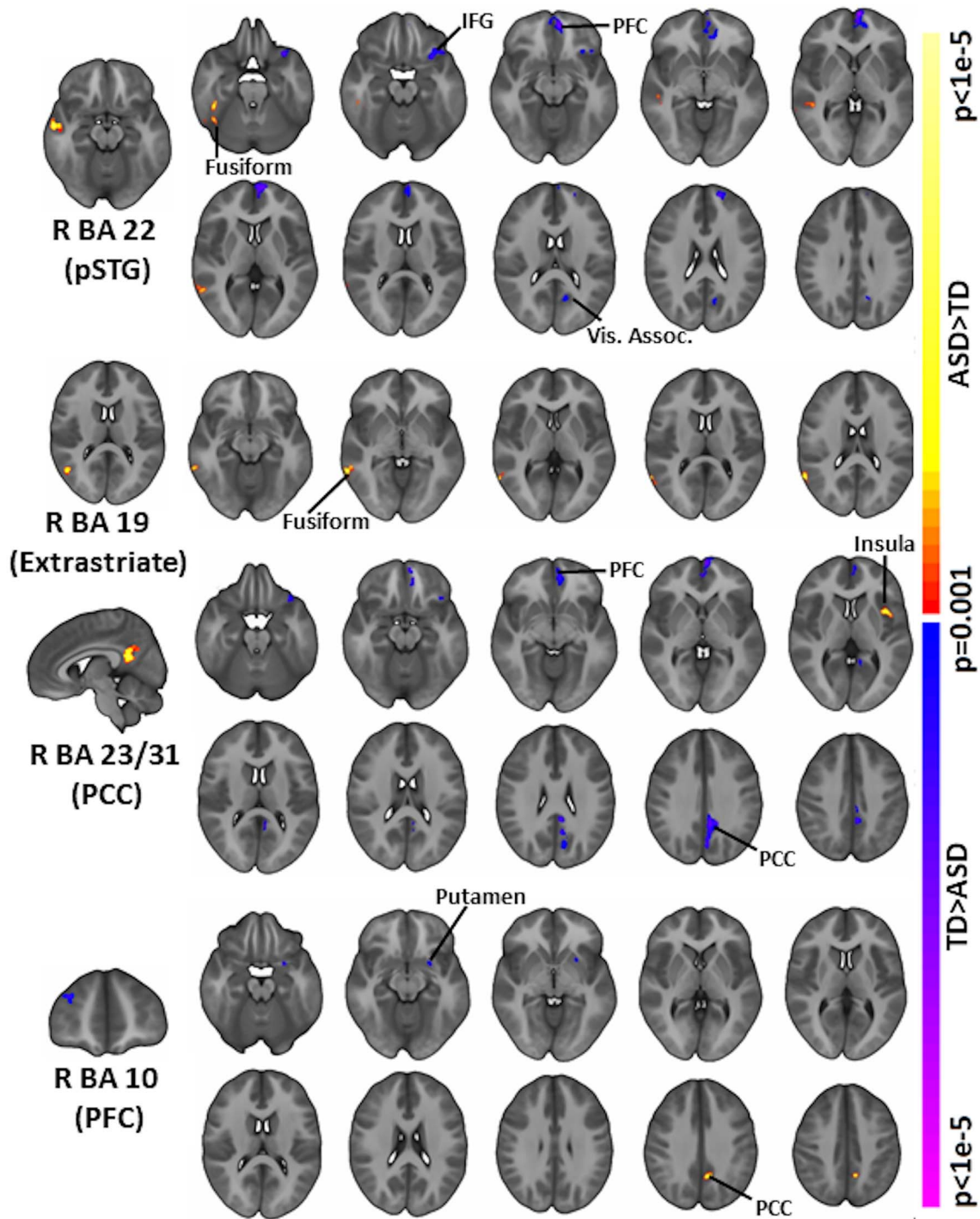


Figure 2. Follow-up seed connectivity. Derived from our main group analysis, we performed follow-up seed connectivity analysis using the pSTG (R BA 22), extrastriate cortex (R BA 19), PCC (R BA 23, R BA 31), and PFC (R BA 10) as seeds. A diverse set of connections and large-scale networks contribute to the group differences observed in Figure 1. Seed regions are shown on the leftmost column. All results shown at $P < 0.05$ corrected and in radiologic convention.

ASD exhibited increased hemispheric asymmetries in the right PCC, the right pSTG, and the right extrastriate cortex but exhibited decreased asymmetries in the right anterior PFC. Follow-up seed connectivity from these regions revealed a diverse set of connections and large-scale networks contributing to this atypical hemispheric specialization. Additionally, two of those

regions (right PCC and right extrastriate) also exhibited atypical hemispheric specialization in 9-month-old HR-nonASD and ASD infants compared to NR infants with similar effect sizes as observed in the school-age sample. HR-nonASD were not significantly different than the infants that later met ASD criteria. Finally, for the extrastriate cortex, the developmental trajectories from 1

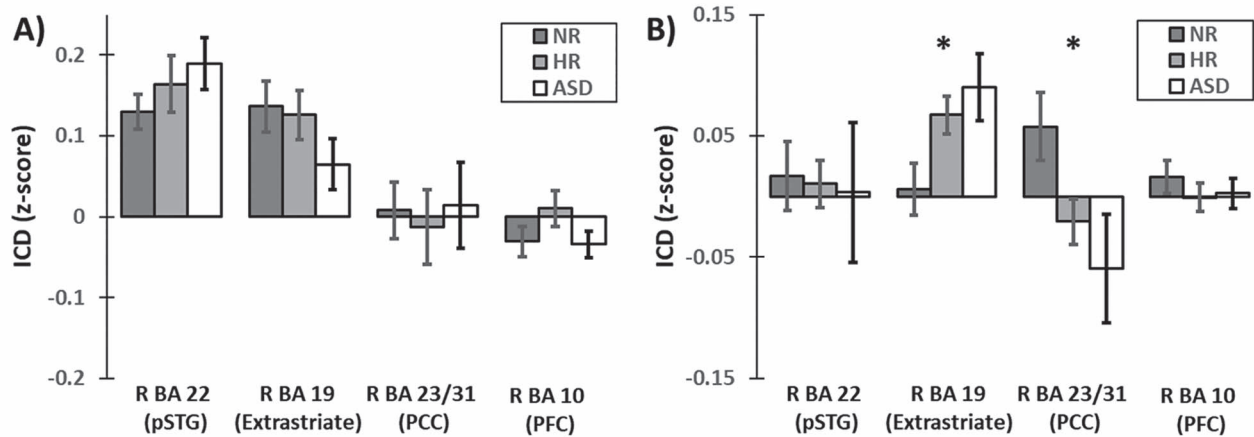


Figure 3. Group differences in connectivity hemispheric specialization in infancy. (A) At 1 month ($n=43$), none of the ROIs from the school-aged sample exhibited significant differences between the infant groups. (B) However, at 9 months ($n=57$), the right extrastriate cortex (BA 19) and right PCC (R BA 23/31) exhibited significant differences in lateralization between the infant groups. Error bars represent standard errors. *denotes significance at $P < 0.05$.

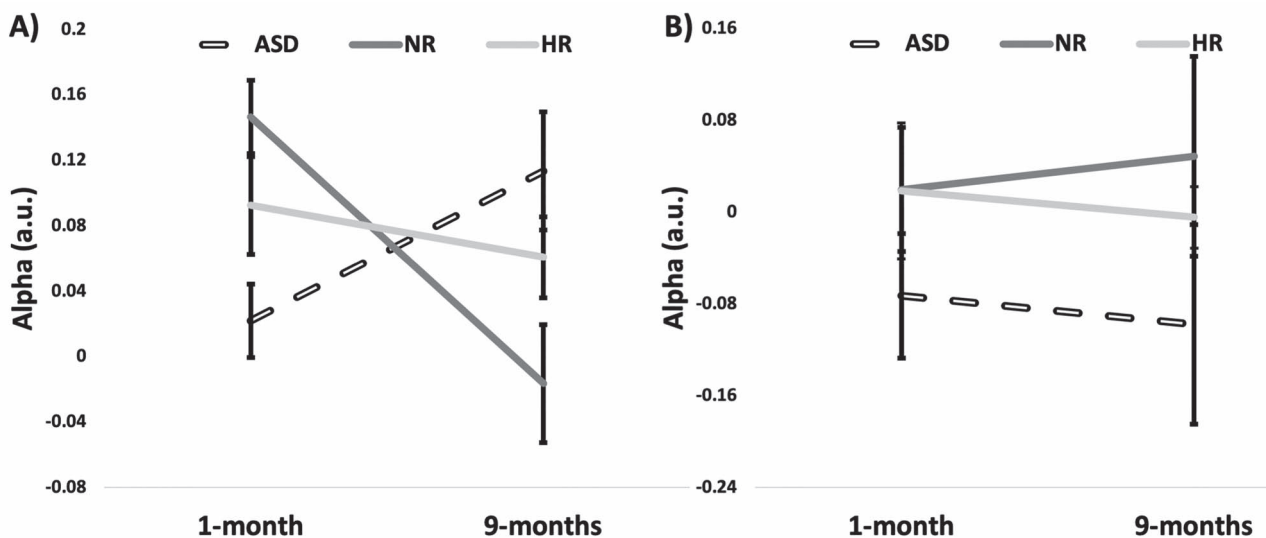


Figure 4. Developmental trajectories from 1 to 9 months for the right extrastriate cortex (BA 19) and PCC in infants with longitudinal data. (A) For the extrastriate cortex, at 1 month, NR and HR-nonASD infants exhibited higher chICD compared to the ASD infants; while, by 9 months, the ASD infants exhibited higher chICD compared to the NR and HR-nonASD infants. The trajectories for the NR infants were significantly different than those for the HR-nonASD and ASD infants. (B) For the PCC, the trajectories were not significantly different between groups. Error bars represent standard errors.

to 9 months were significantly different between the NR infants and the HR-nonASD and ASD infants. Overall, these differences come online in parallel with those observed on the neurobehavioral (Jones and Klin 2013) and neurostructural (Wolff et al. 2015; Eggebrecht et al. 2017; Emerson et al. 2017; Lewis et al. 2017; Shen et al. 2017) levels and precede the emergence of behavioral symptoms.

Alterations in the connectivity of the DMN were the most prominent of our results. Three of the four regions identified in the older children (PCC, extrastriate, and pSTG) and both regions in the infants (PCC and extrastriate) are part of the DMN, a large-scale brain network critically involved in self-referential thinking. The DMN—especially, in the context of its interactions with other large-scale brain networks—is a major contributor in the etiology of ASD (Padmanabhan et al. 2017). While hemispheric specialization of the DMN has not been

widely investigated, the few existing studies suggest that hemispheric asymmetries are decreased in the PCC in school-aged children (Nielsen et al. 2014; Lee et al. 2016). In general, the PCC demonstrates weaker connectivity in children and young adults with ASD (Rane et al. 2015). Notably, in the infant sample, the PCC hemispheric asymmetries for the HR-nonASD were in-between the values of the LR and ASD infants, suggesting that atypical DMN patterns (though of less magnitude) may also be observed in those at high genetic risk for ASD. This result is also consistent with the observation that, while less than 20% of siblings will receive an ASD diagnosis, a much larger percent will show a broader autism phenotype or may have deficits in language and social processing (Ozonoff et al. 2011).

In line with this and prior studies (Rane et al. 2015), our seed connectivity results demonstrate altered connectivity between

the PCC and the insula and the PCC and the PFC in individuals with ASD. The insula and PFC regions detected in the chICD analysis are key nodes of the salience network. The salience network plays a role in detecting salient stimuli and in orienting attentional resources to them (Seeley et al. 2007). Together, altered connectivity between DMN and salience network, putatively, contributes to reduced flexibility to attend to social stimuli and altered integration of information about the self in reference to others in individuals with ASD (Padmanabhan et al. 2017).

The PCC appears to undergo large changes in the hemispheric specialization between infancy and school-age as patterns of group differences are reversed in the two samples and as there were no significant differences in the infant PCC trajectories. Given that the anterior portion of DMN (i.e., PCC connectivity) is putatively one of the last large-scale brain networks to mature (Gao et al. 2009), it may not be all that surprising to observe these results. Divergence between infant studies and studies in older children is often attributed to the rapid growth of the brain in infancy followed by pruning processes in later childhood (Spann et al. 2020). This fact would be consistent with the larger chICD value observed in TD infants compared to the TD school-aged children. While the strength of these connections may vary based on age, the patterns of group differences demonstrated that within an age group, such as the findings with extrastriate connectivity (e.g., increased asymmetry in individuals with ASD classification compared to peers), are markedly consistent for the infant and school-age samples.

Notably, between 1 and 9 months of age, infants are beginning to develop many of the social skills associated with DMN and salience network interactions (Fenoglio et al. 2017). During this period, infants undergo several pivotal transitions to engage with their caregiver and environment (Shultz et al. 2018). Neonates demonstrate reflex-like attunement to their social environment, demonstrating reflexive crying, orientation to faces and visual tracking, and arms in asymmetrical tonic neck reflex position (Shultz et al. 2018). Over the first 6 months of life, reflexes are gradually replaced with volitional action and skills that progressively build upon each other and increase in complexity as infants increasingly interact with others and environment. For example, reflexive eye-looking is replaced with volitional, social-interactional eye-looking, and reflexive arm positioning and palmar grasp reflexes are replaced with reaching and grasping behavior and eventually social waving (Shultz et al. 2018). In infants that later develop ASD, the progression of these developmental skills has been noted to be disrupted (Zwaigenbaum et al. 2005; Bhat et al. 2012; Jones and Klin 2013; LeBarton and Iverson 2016).

The extrastriate cortex, for which ASD infants exhibited a significantly different developmental trajectory from 1 to 9 months compared to NR infants, is involved in many aspects of visual proceeding, including the perception of other people's body parts and the observer's body parts during goal-directed movements. Thus, tracking how alterations in hemispheric asymmetries associate with alterations in social skills remains an important next step in understanding the developmental impact of these differences in ASD.

When investigating neurodevelopmental disorders, it remains critical to know when group differences emerge (Wolff et al. 2015). Understanding these critical and/or sensitive periods may provide insight to the etiological pathways and inform eventual interventions (Voss 2013). While comparisons between two different cohorts (such as this study) does not allow us to precisely probe when all the observed differences emerge,

it does allow us to narrow the "search window." For example, the school-age results alone only provide evidence that these differences emerge sometime within the first decade of life. However, by including longitudinal infant data, we provide evidence that altered hemispheric specialization of the DMN emerges within the first year of life.

While an ideal case is to have longitudinal data from infancy through school-age, these studies are expensive, take decades to perform, and rarely collect sample sizes comparable to our study ($n > 800$). Studies that merge independent data from diverse samples are a powerful and needed alternative. Importantly, by using a second dataset, we provide evidence that our results in the school-age children are generalizable and robust. For any marker of ASD diagnosis to have eventual clinical utility, it must generalize in independent data and be robust to factors, like data acquisition and participant recruitment.

Our results and other studies (Wolff et al. 2015; Eggebrecht et al. 2017; Emerson et al. 2017; Lewis et al. 2017; Shen et al. 2017) suggest that multiple, infant markers of future ASD diagnosis may exist from a wide range of neuroimaging data (Wolff et al. 2015; Eggebrecht et al. 2017; Emerson et al. 2017; Lewis et al. 2017; Shen et al. 2017). Given the heterogeneity in ASD, likely, the best markers will come from ensemble methods that can integrate information from all of these and incorporate markers from different ages. Future work should investigate how to combine multiple modalities to not only improve potential clinical utility but also to better capture the neurodevelopmental etiology of ASD.

Strengths and Limitations

The primary strengths of this work include data-driven methods and imaging data from both infants and older children. Our study has several limitations that should be noted. 1) While we highlight that a proportion of group differences between children with ASD and TD peers are observable in infancy using longitudinal infant imaging data, we lack longitudinal data from infancy to school-age. As a result, we cannot pinpoint when the remaining group differences emerge. 2) We excluded many children ($n = 121$) for high head motion during scanning. While minimizing motion related confounds is the best practice in connectivity studies, it may introduce biases and reduce generalization. All school-age participants had IQs in the normal range. Additionally, all school-age children and infants included were able to provide high-quality fMRI data. These factors may not be representative of the broader population and may limit the generalizability of the findings to a broader ASD population. 3) A relatively small number of infants ($n = 43$ at 1 month and $n = 57$) were included in the study, particularly those later diagnosed with ASD, which limits our power to detect group differences between the HR-nonASD and ASD groups despite medium effect sizes. 4) To increase maximize our sample size, we used two different criteria for classifying infants into the ASD group. While these two criteria show good convergence (Luyster et al. 2009), incongruent classification between the measures can exist and limit interpretations (especially between the HR-nonASD and ASD groups). 5) The neuronal-hemodynamic coupling is likely different in infancy compared to school-age (Anderson et al. 2001; Kozberg and Hillman 2016), which limits direct comparisons between the infant and school-age results. Despite these differences, simultaneous electroencephalography fMRI data in infants highlight a tight neuronal-hemodynamic coupling (Arichi et al. 2017), suggesting that—even in infants—fMRI represents a reasonable tool for

studying brain functions. 6) We used a targeted—rather than a whole-brain—approach to investigate group differences in the infants to maximize power. With a larger sample and a whole-brain approach, other regions exhibiting group differences may emerge. We did not detect group differences at 1 month of age. Yet, cellular and molecular studies suggest that altered developmental trajectory start in the fetal period (Willsey et al. 2013). A larger sample of younger infants than in our study is likely needed to detect these differences. 7) We did not detect group differences between ASD and HRnon-ASD infants at 9 months. The lack of differences is likely a power issue as the observed effect size for this contrast were in the medium effect size range. We hypothesize that significant differences between ASD and HRnon-ASD infants at 9 months would be observable in a larger sample. 8) We also did not detect associations between ADOS calibrated severity score and the patterns of atypical cerebral lateralization in either the school-age or infant sample. These atypical patterns may represent group differences that do not scale with symptom severity. However, more nuanced behavioral measures may be beneficial to understand specific symptom profiles contributing to the ASD phenotype.

Conclusions

Children with ASD demonstrate atypical patterns of hemispheric specialization of the DMN and altered seed connectivity to multiple large-scale brain networks compared to their TD peers. Notably, at 9 months—but not 1 month—of age, infants who later received a diagnosis of ASD as well as high-risk infants demonstrate similar patterns in the PCC and extrastriate cortex. Together, these results suggest that differences in hemispheric specialization associated with ASD are present in infancy. Though, their role in etiology of ASD remains to be elucidated. Future studies should continue to clarify the development of these hemispheric specialization differences through longitudinal studies into toddlerhood and older children, potentially identifying predictive markers of ASD through predictive modeling methods.

Supplementary Material

[Supplementary material](#) can be found at *Cerebral Cortex* online.

Disclosures

All authors reported no biomedical financial interests.

Author's contributions

M.R. and D.S. designed the work; M.R., C.L., and D.S. analyzed the data; M.R., K.C., M.S., and D.S. interpreted the data. M.R. and D.S. drafted the article. All authors revised it critically for important intellectual content and approved the version to be published; and they agree to be accountable for all aspects of the work in ensuring that questions related to the accuracy or integrity of any part of the work are appropriately investigated and resolved.

Notes

Vernon W. Lippard, M.D., Student Summer Research Fellowship in Pediatrics (to M.R.); National Institute of Mental Health (NIMH) P50MH115716 (K.C.); NIMH K23MH087770 (DiMartino); Leon Levy

Foundation (DiMartino); NIMH 5R21MH107045 (DiMartino, Milham); NIMH R03MH096321 (Milham); Nathan S. Kline Institute of Psychiatric Research (Milham), Gifts from Joseph P. Healy, Stavros Niarchos Foundation, and Phyllis Green and Randolph Cowen to the Child Mind Institute (Milham). *Conflict of Interest*: None declared.

References

- Anderson AW, Marois R, Colson ER, Peterson BS, Duncan CC, Ehrenkranz RA, Schneider KC, Gore JC, Ment LR. 2001. Neonatal auditory activation detected by functional magnetic resonance imaging. *Magn Reson Imaging*. 19:1–5.
- Anderson JS, Druzgal TJ, Froehlich A, DuBray MB, Lange N, Alexander AL, Abildskov T, Nielsen JA, Cariello AN, Cooper-rider JR et al. 2011. Decreased interhemispheric functional connectivity in autism. *Cereb Cortex*. 21:1134–1146.
- Arichi T, Whitehead K, Barone G, Pressler R, Padormo F, Edwards AD, Fabrizi L. 2017. Localization of spontaneous bursting neuronal activity in the preterm human brain with simultaneous EEG-fMRI. *Elife*. 6:e27814.
- Bhat AN, Galloway JC, Landa RJ. 2012. Relation between early motor delay and later communication delay in infants at risk for autism. *Infant Behav Dev*. 35:838–846.
- Cardinale RC, Shih P, Fishman I, Ford LM, Muller RA. 2013. Pervasive rightward asymmetry shifts of functional networks in autism spectrum disorder. *JAMA Psychiat*. 70:975–982.
- Di Martino A, O'Connor D, Chen B, Alaerts K, Anderson JS, Assaf M, Balsters JH, Baxter L, Beggiato A, Bernaerts S et al. 2017. Enhancing studies of the connectome in autism using the autism brain imaging data exchange II. *Sci Data*. 4:170010.
- Di Martino A, Yan CG, Li Q, Denio E, Castellanos FX, Alaerts K, Anderson JS, Assaf M, Bookheimer SY, Dapretto M et al. 2014. The autism brain imaging data exchange: towards a large-scale evaluation of the intrinsic brain architecture in autism. *Mol Psychiatry*. 19:659–667.
- Dubois J, Hertz-Pannier L, Cachia A, Mangin JF, Le Bihan D, Dehaene-Lambertz G. 2009. Structural asymmetries in the infant language and sensori-motor networks. *Cereb Cortex*. 19:414–423.
- Edgar JC, Fisk CL IV, Berman JI, Chudnovskaya D, Liu S, Pandey J, Herrington JD, Port RG, Schultz RT, Roberts TP. 2015. Auditory encoding abnormalities in children with autism spectrum disorder suggest delayed development of auditory cortex. *Mol Autism*. 6:69.
- Eggebrecht AT, Elison JT, Feczko E, Todorov A, Wolff JJ, Kandala S, Adams CM, Snyder AZ, Lewis JD, Estes AM et al. 2017. Joint attention and brain functional connectivity in infants and toddlers. *Cereb Cortex*. 27:1709–1720.
- Emerson RW, Adams C, Nishino T, Hazlett HC, Wolff JJ, Zwaigenbaum L, Constantino JN, Shen MD, Swanson MR, Elison JT et al. 2017. Functional neuroimaging of high-risk 6-month-old infants predicts a diagnosis of autism at 24 months of age. *Sci Transl Med*. 9(393):eaag2882.
- Fair DA, Dosenbach NU, Church JA, Cohen AL, Brahmbhatt S, Miezin FM, Barch DM, Raichle ME, Petersen SE, Schlaggar BL. 2007. Development of distinct control networks through segregation and integration. *Proc Natl Acad Sci U S A*. 104:13507–13512.
- Fenoglio A, Georgieff MK, Elison JT. 2017. Social brain circuitry and social cognition in infants born preterm. *J Neurodev Disord*. 9:27.

- Floris DL, Barber AD, Nebel MB, Martinelli M, Lai MC, Crocetti D, Baron-Cohen S, Suckling J, Pekar JJ, Mostofsky SH. 2016. Atypical lateralization of motor circuit functional connectivity in children with autism is associated with motor deficits. *Mol Autism*. 7:35.
- Floris DL, Wolfers T, Zabihi M, Holz NE, Zwiers MP, Charman T, Tillmann J, Ecker C, Dell'Acqua F, Banaschewski T et al. 2021. Atypical brain asymmetry in autism—a candidate for clinically meaningful stratification. *Biol Psychiatry Cogn Neurosci Neuroimaging*. 6(8):802–812.
- Gao W, Zhu H, Giovanello KS, Smith JK, Shen D, Gilmore JH, Lin W. 2009. Evidence on the emergence of the brain's default network from 2-week-old to 2-year-old healthy pediatric subjects. *Proc Natl Acad Sci U S A*. 106: 6790–6795.
- Gotts SJ, Simmons WK, Milbury LA, Wallace GL, Cox RW, Martin A. 2012. Fractionation of social brain circuits in autism spectrum disorders. *Brain*. 135:2711–2725.
- Greicius MD, Krasnow B, Reiss AL, Menon V. 2003. Functional connectivity in the resting brain: a network analysis of the default mode hypothesis. *Proc Natl Acad Sci U S A*. 100: 253–258.
- Habas PA, Scott JA, Roosta A, Rajagopalan V, Kim K, Rousseau F, Barkovich AJ, Glenn OA, Studholme C. 2012. Early folding patterns and asymmetries of the normal human brain detected from in utero MRI. *Cereb Cortex*. 22:13–25.
- Jones W, Klin A. 2013. Attention to eyes is present but in decline in 2-6-month-old infants later diagnosed with autism. *Nature*. 504:427–431.
- Joshi A, Scheinost D, Okuda H, Belhachemi D, Murphy I, Staib LH, Papademetris X. 2011. Unified framework for development, deployment and robust testing of neuroimaging algorithms. *Neuroinformatics*. 9:69–84.
- Kleinhans NM, Muller RA, Cohen DN, Courchesne E. 2008. Atypical functional lateralization of language in autism spectrum disorders. *Brain Res*. 1221:115–125.
- Kozberg M, Hillman E. 2016. Neurovascular coupling and energy metabolism in the developing brain. *Prog Brain Res*. 225:213–242.
- LeBarton ES, Iverson JM. 2016. Associations between gross motor and communicative development in at-risk infants. *Infant Behav Dev*. 44:59–67.
- Lee HW, Arora J, Papademetris X, Tokoglu F, Negishi M, Scheinost D, Farooque P, Blumenfeld H, Spencer DD, Constable RT. 2014. Altered functional connectivity in seizure onset zones revealed by fMRI intrinsic connectivity. *Neurology*. 83:2269–2277.
- Lee JM, Kyeong S, Kim E, Cheon KA. 2016. Abnormalities of inter- and intra-hemispheric functional connectivity in autism spectrum disorders: a study using the autism brain imaging data exchange database. *Front Neurosci*. 10:191.
- Lewis JD, Evans AC, Pruett JR Jr, Botteron KN, McKinstry RC, Zwaigenbaum L, Estes AM, Collins DL, Kostopoulos P, Gerig G et al. 2017. The emergence of network inefficiencies in infants with autism spectrum disorder. *Biol Psychiatry*. 82:176–185.
- Lord C, Petkova E, Hus V, Gan W, Lu F, Martin DM, Ousley O, Guy L, Bernier R, Gerds J et al. 2012. A multisite study of the clinical diagnosis of different autism spectrum disorders. *Arch Gen Psychiatry*. 69:306–313.
- Lord C, Rutter M, DiLavore P, Risi S, Gotham K, Bishop S. 2012. *Autism diagnostic observation schedule—2nd edition (ADOS-2)*. Los Angeles (CA): Western Psychological Corporation.
- Lord C, Rutter M, DiLavore PC, Risi S. 2002. *Autism diagnostic observation schedule—WPS (ADOS-WPS)*. Los Angeles (CA): Western Psychological Services.
- Luyster R, Gotham K, Guthrie W, Coffing M, Petrak R, Pierce K, Bishop S, Esler A, Hus V, Oti R et al. 2009. The autism diagnostic observation schedule-toddler module: a new module of a standardized diagnostic measure for autism spectrum disorders. *J Autism Dev Disord*. 39: 1305–1320.
- Maenner MJ, Shaw KA, EdS BJ, Washington A, Patrick M, DiRienzo M, Christensen DL, Wiggins LD, Pettygrove S, Andrews JG et al. 2020. Prevalence of autism spectrum disorder among children aged 8 years—autism and developmental disabilities monitoring network, 11 sites, United States, 2016. *MMWR Surveill Summ*. 69:1–12.
- Nielsen JA, Zielinski BA, Fletcher PT, Alexander AL, Lange N, Bigler ED, Lainhart JE, Anderson JS. 2014. Abnormal lateralization of functional connectivity between language and default mode regions in autism. *Mol Autism*. 5:8.
- Ozonoff S, Young GS, Carter A, Messinger D, Yirmiya N, Zwaigenbaum L, Bryson S, Carver LJ, Constantino JN, Dobkins K et al. 2011. Recurrence risk for autism spectrum disorders: a Baby Siblings Research Consortium study. *Pediatrics*. 128:e488–e495.
- Ozonoff S, Young GS, Landa RJ, Brian J, Bryson S, Charman T, Chawarska K, Macari SL, Messinger D, Stone WL. 2015. Diagnostic stability in young children at risk for autism spectrum disorder: a Baby Siblings Research Consortium study. *J Child Psychol Psychiatry*. 56:988–998.
- Padmanabhan A, Lynch CJ, Schaer M, Menon V. 2017. The default mode network in autism. *Biol Psychiatry Cogn Neurosci Neuroimaging*. 2:476–486.
- Rane P, Cochran D, Hodge SM, Haselgrove C, Kennedy DN, Frazier JA. 2015. Connectivity in autism: a review of MRI connectivity studies. *Harv Rev Psychiatry*. 23:223–244.
- Redcay E, Courchesne E. 2008. Deviant functional magnetic resonance imaging patterns of brain activity to speech in 2-3-year-old children with autism spectrum disorder. *Biol Psychiatry*. 64:589–598.
- Rudolph MD, Graham AM, Feczko E, Miranda-Dominguez O, Rasmussen JM, Nardos R, Entringer S, Wadhwa PD, Buss C, Fair DA. 2018. Maternal IL-6 during pregnancy can be estimated from newborn brain connectivity and predicts future working memory in offspring. *Nat Neurosci*. 21: 765–772.
- Satterthwaite TD, Elliott MA, Gerraty RT, Ruparel K, Loughead J, Calkins ME, Eickhoff SB, Hakonarson H, Gur RC, Gur RE et al. 2013. An improved framework for confound regression and filtering for control of motion artifact in the preprocessing of resting-state functional connectivity data. *Neuroimage*. 64:240–256.
- Scheinost D, Kwon SH, Lacadie C, Vohr BR, Schneider KC, Papademetris X, Constable RT, Ment LR. 2017. Alterations in anatomical covariance in the prematurely born. *Cereb Cortex*. 27:534–543.
- Scheinost D, Kwon SH, Shen X, Lacadie C, Schneider KC, Dai F, Ment LR, Constable RT. 2016. Preterm birth alters neonatal, functional rich club organization. *Brain Struct Funct*. 221:3211–3222.
- Scheinost D, Lacadie C, Vohr BR, Schneider KC, Papademetris X, Constable RT, Ment LR. 2015. Cerebral lateralization is protective in the very prematurely born. *Cereb Cortex*. 25(7): 1858–66.

- Scheinost D, Papademetris X, Constable RT. 2014. The impact of image smoothness on intrinsic functional connectivity and head motion confounds. *Neuroimage*. 95: 13–21.
- Scheinost D, Tokoglu F, Hampson M, Hoffman R, Constable RT. 2019. Data-driven analysis of functional connectivity reveals a potential auditory verbal hallucination network. *Schizophr Bull*. 45(2):415–424.
- Seeley WW, Menon V, Schatzberg AF, Keller J, Glover GH, Kenna H, Reiss AL, Greicius MD. 2007. Dissociable intrinsic connectivity networks for salience processing and executive control. *J Neurosci Off J Soc Neurosci*. 27:2349–2356.
- Shen MD, Kim SH, McKinstry RC, Gu H, Hazlett HC, Nordahl CW, Emerson RW, Shaw D, Elison JT, Swanson MR et al. 2017. Increased extra-axial cerebrospinal fluid in high-risk infants who later develop autism. *Biol Psychiatry*. 82: 186–193.
- Shultz S, Klin A, Jones W. 2018. Neonatal transitions in social behavior and their implications for autism. *Trends Cogn Sci*. 22:452–469.
- Spann MN, Bansal R, Hao X, Rosen TS, Peterson BS. 2020. Prenatal socioeconomic status and social support are associated with neonatal brain morphology, toddler language and psychiatric symptoms. *Child Neuropsychol*. 26:170–188.
- Tomasi D, Volkow ND. 2019. Reduced local and increased long-range functional connectivity of the thalamus in autism Spectrum disorder. *Cereb Cortex*. 29:573–585.
- Voss P. 2013. Sensitive and critical periods in visual sensory deprivation. *Front Psychol*. 4:664.
- Wang D, Buckner RL, Liu H. 2014. Functional specialization in the human brain estimated by intrinsic hemispheric interaction. *J Neurosci*. 34:12341–12352.
- Willsey AJ, Sanders SJ, Li M, Dong S, Tebbenkamp AT, Muhle RA, Reilly SK, Lin L, Fertuzinhos S, Miller JA et al. 2013. Coexpression networks implicate human midfetal deep cortical projection neurons in the pathogenesis of autism. *Cell*. 155:997–1007.
- Wolff JJ, Gerig G, Lewis JD, Soda T, Styner MA, Vachet C, Botteron KN, Elison JT, Dager SR, Estes AM et al. 2015. Altered corpus callosum morphology associated with autism over the first 2 years of life. *Brain*. 138:2046–2058.
- Zwaigenbaum L, Bryson S, Rogers T, Roberts W, Brian J, Szatmari P. 2005. Behavioral manifestations of autism in the first year of life. *Int J Dev Neurosci*. 23:143–152.